TEMPERATURE MODELLING OF AN HOMOGENEOUS MEDIUM USING GENETICALLY SELECTED RBF(LIC)

C. A. Teixeira * **M. Graça Ruano** *
W. C. A. Pereira ** **A. E. Ruano** *

* *Centre for Intelligent Systems, FCT, University of Algarve, Portugal*
** *PEB-COPPE, Federal University of Rio de Janeiro, Brazil*

Abstract: Temperature modelling of human tissue exposed to therapeutic ultrasound is essential for an accurate instrumental assessment and calibration. In this paper punctual temperature modelling of an homogeneous medium, radiated by therapeutic ultrasound, is presented. Two different approaches are considered: a completely nonlinear approach (Radial Basis Functions neural networks (RBF)), and a hybrid (Linear plus nonlinear) approach (Radial Basis Functions neural networks with Linear Input Connections (RBFLIC)). The best-performant Neural Network (NN) structures were obtained using a Multi-Objective Genetic Algorithm (MOGA). The best RBFLIC structure for the applied MOGA parametrisation, presents 28% improvement in the performance of the best RBF structure.

Keywords: Biomedical systems, Temperature profiles, Neural network-models, Radial base function networks, Multiobjective optimisations.

1. INTRODUCTION

The lack of reliable human tissue models conditions a broader use of therapeutic ultrasound instrumentation. The existence of precise and effective tissue temperature variation models together with fine tuned instrumental control, will provide usage of ultrasound therapy on small areas, depth controlled, and cellular targeted applications.
Having in mind non-invasive temperature estimation in time and space, previous work in the area considers that the changes in temperature are linearly related with the changes in sound velocity and with the medium expansion, achieving a maximum absolute error of 0.44^oC, an average error of -0.02^oC, and a mean squared error of $0.03(^oC)^2$. These error values were obtained with experiments were the temperature ranged between $20.5^oC$and 24.5^oC(Simon *et al.*, 1998). There is also work reporting this kind of non-invasive estimation applied to therapeutic instrumentation control(Seip *et al.*, 1996).
Previous studies of our research group in punctual and nonlinear temperature modelling, considered RBF to estimate the temperature in a homogeneous medium, when it is irradiated by therapeutic ultrasound. The values of the fundamental component of the intensity spectrum, and the past temperature values were considered relevant RBF inputs. The maximum absolute error obtained so far was 0.2^oC, in a temperature range between $31^oC$and 38.8^oC(Teixeira *et al.*, 2004).
The work hereby presented, considers similar experimental conditions of (Teixeira *et al.*, 2004) but the temperature modelling is now performed by a completely nonlinear approach (RBF), and

Table 1. Temperature ranges.

Intensity	Temperature (^oC)		
($Watt/cm^2$)	Initial	Max.	Final
1	29	34.5	28.5
1.5	30	37.2	28
2	31	38.8	31

compared with a hybrid approach (RBFLIC). The values of the fundamental component of the intensity spectrum, associated harmonics, and the past temperature values are inputs of the RBF(LIC).

2. EXPERIMENTAL SETUP

Temperature and acoustic intensity signals, measured in a 48 mm axially distant point from an ultrasonic therapeutic probe submerged in a glycerin tank (homogeneous medium) are the data considered in this work. Data was acquired during approximately 110 min. At each 10 seconds, a discrete value of the temperature waveform was acquired, as well as a $5\mu s$ wide window of the acoustic intensity signal. That window corresponds to 2000 points of the intensity waveform. Mechanical energy was supplied only in the first 60 min, by the ultrasonic therapeutic device (Ibramed Sonopulse (São Paulo)), since in the last 50 minutes the acoustical energy was maintained at zero level. Three sets of signals were acquired at 3 MHz in continuous operating mode, at three different intensities: $1Watt/cm^2$, $1.5Watt/cm^2$ and $2Watt/cm^2$. The initial, maximum, and final temperature of the glycerin medium in the point of interest are summarised in Table 1. The experimental arrangement is described in Fig. 1.

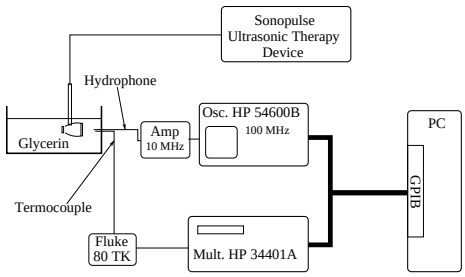

Fig. 1. Experimental setup.

3. METHODS

3.1 Processing the experimental data

From the intensity signals collected from the experiment, some spectral features were extracted aiming the development of the temperature models. After a *Fast Fourier Transform* computation the amplitude of the fundamental component (≈3 MHz), of the first harmonic (≈6MHz), and of the second harmonic (≈9MHz) were saved for future use in the RBF(LIC) training, test and validation. In a posterior phase, the feature extracted and the measured temperature signals were normalised between 0 and 1, in order to eliminate the differences in scale between the variables, having as objective the correct training of the NNs. The convention used for the remaining text is the following: normalised amplitude of the fundamental component - I_{fc}, normalised amplitude of the first harmonic - I_{1h}, normalised amplitude of the second harmonic - I_{2h}, and normalised temperature - T.
At the end of this process we selected the data collected at $1Watt/cm^2$ for training, the data collected at $1.5Watt/cm^2$ for test, and the data collected at $2Watt/cm^2$ for validation. The training, test, and validation sets are composed by 429, 427, and 400 patterns, respectively.

3.2 RBF and RBFLIC

A RBF consists of a three fully connected layered NN. The first layer is a set of inputs, the second is formed by a set of processing elements, called neurons, which perform a nonlinear transformation on the input data. The last layer combines linearly the output of the hidden layer to compute the overall network output. The input/output (I/O) relation for a RBF is given by:

$$f(x_j) = b + \sum_{i=1}^{n} \alpha_i \varphi\left(||x_j - c_i||\right) \qquad (1)$$

where n is the number of neurons in the hidden layer, b is the bias term, $||.||$ is an Euclidean norm, and $\varphi\left(||x_j - c_i||\right)$ is a set of nonlinear radial basis functions weighted by $\{\alpha_i\}_{i=1}^{n}$. The basis functions are centred at $\{c_i\}_{i=1}^{n}$ (centres) and are evaluated at points x_j. Usually these functions are Gaussian:

$$\varphi_i = e^{\frac{1}{2\sigma_i^2}||x_j - c_i||^2} \qquad (2)$$

An RBFLIC (Fig. 2) is formed by a normal RBF plus a set of linear input connections. The I/O relation for this network is given by:

$$f_{LIC}(x_j, xl_j) = b + \sum_{i=1}^{n} \alpha_i \varphi\left(||x_j - c_i||\right) + \sum_{k=1}^{l} \lambda_k xl_{jk} \qquad (3)$$

where $\{xl_{jk}\}_{k=1}^{l}$ is the set of linear inputs, and $\{\lambda_k\}_{k=1}^{l}$ are the associated weights.

3.3 Multi-objective Genetic Algorithm (MOGA)

In the construction of a RBF(LIC) several questions arises: What is the appropriate number of

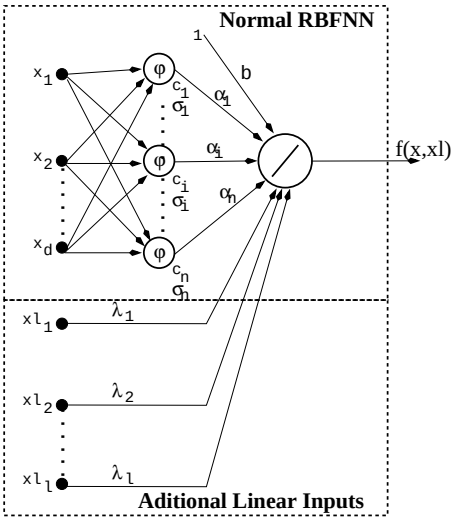

Fig. 2. RBFLIC topology.

neurons that produces the smallest error? Which are the important input variables for a good model? What are the important lags of those variables?(Ferreira *et al.*, 2003) Which lagged variables should be used as additional linear inputs, and which ones should be inputs to the neurons?

To answer these questions a MOGA (Fonseca and Fleming, 1993) was used to select the best fitted RBF structures (Ferreira *et al.*, 2003). In this work the same approach was extended to the RBFLIC case. The important variables considered were: the spectral features referred in 3.1 (I_{fc}, I_{1h}, and I_{2h}), and the past values of T. In order to define the MOGA search space, the number of inputs was restricted to a maximum of 20 for the RBF case, and 20 linear and nonlinear inputs for the RBFLIC case. The number of neurons was restricted to the interval $[2, 15]$ for both topologies, and the maximum admissible lag (MLAG) was defined to be 20. In this particular case MOGA ran during 100 generations, of 100 RBF(LIC) (individuals) each. The crossover and mutations probabilities were defined as 0.7 and 0.5 respectively. To maintain population diversity in each generation, 10% of the population was changed by a randomly generated set of individuals. The previously referred values were the ones that produced the best MOGA results, and were selected after several tests, considering different parameter arrangements.

3.3.1. Computation of individuals performance

The training of each individual was performed using the Levenberg Marquardt (LM) algorithm with the "early-stopping" termination criteria (Ferreira *et al.*, 2002). At each iteration the LM optimised only the values of the centres and spreads, while the linear parameters ($\{\alpha_i\}_{i=1}^{n}$ and $\{\lambda_k\}_{k=1}^{l}$) were obtained using the "Least Squares"(LS) strategy(Ferreira *et al.*, 2002). This approach reflects a nonlinear-linear structure as found on RBF NNs. The initial values of the centres and spreads were determined using the optimal k-means algorithm (Chinrungrueng and Séquin, 1995).

After training, the performance of each individual was accessed according to the following measures:

- Root Mean Square Error in the TRaining set (RMSETR)
- Root Mean Square Error in the TEst set (RMSETE)
- Model-validity tests
- Model ComPlexity (MCP)

The model-validity tests considered are described in (Billings and Voon, 1986), (Billings and Zhu, 1993), and used in (Ferreira *et al.*, 2003). These tests involve the computation of auto-correlation, cross-correlation and higher correlations functions involving model residuals, inputs, and outputs. If the fitted model is adequate, the following conditions should hold:

$$\begin{aligned} R_{ee}(\tau) &= \delta(\tau) \\ R_{ue}(\tau) &= 0 \quad ,\forall\tau \\ R_{u^{2\prime}e}(\tau) &= 0 \quad ,\forall\tau \\ R_{u^{2\prime}e^2}(\tau) &= 0 \quad ,\forall\tau \\ R_{e(eu)}(\tau) &= 0 \quad ,\tau \geq 0 \\ R_{e^2e^2}(\tau) &= \delta(\tau) \\ R_{(ye)e^2}(\tau) &= k\delta(\tau) \\ R_{(ye)u^2}(\tau) &= 0 \quad ,\forall\tau \end{aligned} \tag{4}$$

In reality, the correlations presented in eq. 4 will never equal zero for all lags. This way, the model is considered adequate if the normalised correlation tests lie within 95% confidence limits, defined as:

$$CI = 1.96/\sqrt{N}, \tag{5}$$

where N is the number of training patterns. In the same way, the autocorrelations of the residuals never match exactly the delta function, but will be considered as adequate if the autocorrelation plot enters the 95% confidence interval before lag one. The MCP is computed as the total number of parameters for a particular NN structure:

$$\text{MCP} = NC \times NLE + NS + NW, \tag{6}$$

where NC is the number of centres, NLE the number of nonlinear entries, NS the number of spreads, and $NW = n + l$ is the number of linear plus nonlinear weights.

3.3.2. MOGA objectives, goals, and priorities

From the MOGA point of view, the RMSETR, RMSETE, maximum of correlation test, and MCP are objectives to minimise. Having in mind the attainment of models with a higher generalisation capacity, the RMSETE was defined as a goal

of priority 2, and with value 0.003. The maximum of the correlation tests were defined with a goal value of $CI = 1.96/\sqrt{429 - \text{MLAG}} = 0.097$, and with priority 1. In order to discard large models of heavy computation, MCP was defined as a goal with priority 1, and value 70. This value was selected having in mind the MOGA search space, defined in sub-section 3.3.

4. RESULTS AND DISCUSSION

In this section the selection of the best individuals from the preferable set, was based in the RMSEV. This means that the best individual is the one presenting the best Root Mean Square Error in the Validation set (RMSEV), when compared to other individuals in the preferable set.
The assumptions made in this section are relative to the present MOGA parametrisation and to the runs presented, discarding any attempt of generalisation.

4.1 RBF

The MOGA run applied for RBF NNs, executed as explained in sub-section 3.3, yielded a non-dominated set with 2552 individuals and a preferable set of 15. From the preferable set the best individual presents a RMSEV of 0.0018, a maximum absolute error of 0.09^oC, a mean squared error of 0.0049 $(^oC)^2$, and an average error of -0.0184 ^oC. This model has 6 neurons, and a weights norm of 4.756. The MOGA objectives for this individual are presented in Table 2. Looking at these values, we can state that this individual fulfils 7 out of 10 goals. However, the goals that are not fulfilled are close to the desired values. The inputs (nonlinear inputs) of this individual are presented in Table 3. Analysing this table we can say that the information from I_{fc} is not of interest for temperature modelling, considering its absence in the input set. The importance of the first harmonic is marked by the presence of 2 lags. The second harmonic information is important for the temperature modelling, taking into account the great number of inputs related to this variable. The past memory of the system (past temperature values) is also relevant for the model. The physical validity of the system can be demonstrated by the presence o the first lag of the temperature variable $(T(k-1))$, showing that the actual temperature is dependent of the temperature in the previous 10 seconds. The temperature in the past 60 seconds (1 minute) is also important for the estimation of the actual temperature $(T(k))$, given the presence of $T(k-6)$. The presence of this lag reflects the thermal capacitance of the glycerin tank.
Fig. 3 shows the absolute frequency of the RBF inputs. Analysis of this figure enables stating that all the RBFs in the preferable set do not have lags of I_{fc}, showing that its absence in the best individual is not accidental. The 1^{st} lag of I_{h1} $(I_{h1}(k-1))$ appears in 13 of the 15 NNs demonstrating its importance for the model. The 6^{th} lag of I_{h2} $(I_{h2}(k-6))$, as well as the 1^{st} lag of T appears in all preferable NNs. The previous statements, and the fact that all the NNs have 6 neurons, demonstrate the convergence of the MOGA for the parameterisation presented in sub-section 3.3.

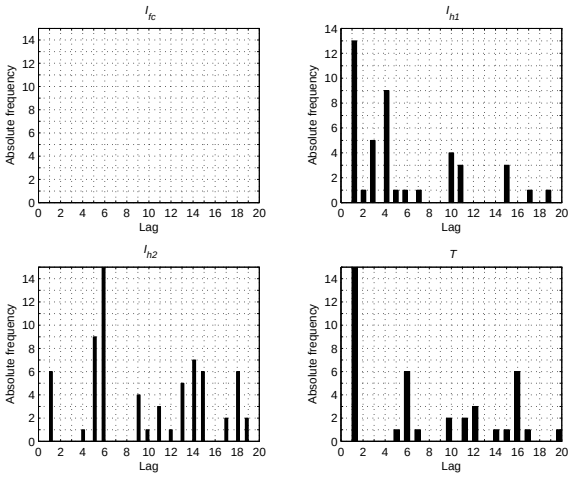

Fig. 3. Absolute frequency of the RBF inputs (preferable set).

Comparing the results in this work, with those presented in (Teixeira *et al.*, 2004), it can be said that the consideration of the 1^{st} and 2^{nd} harmonics of the intensity spectrum as inputs together with the additional objectives introduced in MOGA, lead to a reduction of the maximum absolute error from 0.2^oC to 0.09^oC. In addition, the information of the fundamental component (I_{fc}) is completely discarded from the preferable set in this work, reflecting that temperature modelling is better achieved when only information of I_{h1}, I_{h2}, and T is considered as inputs.

4.2 RBFLIC

MOGA was applied to RBFLIC, yielding a non-dominated set of 2902 individuals, and a preferred set of 20. The best individual presents a RMSEV of 0.0014, a maximum absolute error of 0.12^oC, a mean squared error of $0.0032(^oC)^2$, and an average error of -0.0047^oC. This model has 3 neurons, and a weight $(||\{\alpha_i\}_{i=1}^{n} + \{\lambda_k\}_{k=1}^{l}||)$ norm of 0.9206. The MOGA optimisation objectives are also presented in Table 2. This individual fulfils 6 out of 10 objectives defined. In the same way as for RBFs, the objectives which are not fulfilled are close to the defined goal. The linear and nonlinear inputs of the best individual are presented

Table 2. Performance of the best RBF(LIC)

	RMSETR	RMSETE	MCP	R_{ee}	$R_{e^2e^2}$	$R_{(ye)e^2}$	$R_{(ye)u^2}$	R_{ue}	$R_{u^2e^2}$	R_{u^2e}	$R_{e(eu)}$
RBF	0.0009	**0.0016**	**61**	**0.0921**	**0.0156**	0.0987	**0.0762**	**0.0869**	0.1080	**0.0762**	0.1046
RBFLIC	0.0009	**0.0014**	**69**	0.1243	**0.0154**	0.1067	**0.0848**	**0.0933**	0.1096	**0.0860**	0.1256
Goal	-	0.003	70	0.097	0.097	0.097	0.097	0.097	0.097	0.097	0.097
Prior.	-	2	1	1	1	1	1	1	1	1	1

Table 3. Inputs of the best RBF(LIC)

	Input type	I_{fc}	I_{h1}	I_{h2}	T
RBF	Nonlinear	-	1,4	5,6,15,18	1,6
RBFLIC	Nonlinear	1,7	7,9,12,15	1,3,6,13	2,7,11,17
	Linear	1,2,6,7	6,8,12,14	6,9,17,18	1,5,7,8,12,14,16,17

in Table 3. From this table it can be stated that the information of I_{fc} is of reduced importance as a non-linear input, since only two lags ($I_{fc}(k-1)$ and $I_{fc}(k-7)$) appeared, as for the RBF run. However, the information of this variable is more important as a linear input. The information of I_{h1} has the same relevance as both nonlinear and linear inputs, given the same number of lags. In addition, those lags are in the same range, between 6 and 15, and are almost mutually exclusives. The past values of T (memory of the system) appears in a great number as linear inputs. The physical validity of the best model can be proved by the presence of the 1^{st} lag of T (temperature value in the past 10 sec.) as a linear input, and the 2^{nd} lag of T as a nonlinear input. The medium and higher lags of the estimated variable are also important in the models, ie. the medium term and long term memory of the system.

Fig. 4 presents the absolute frequency, in the preferable set, of the nonlinear and linear inputs of the RBFLIC. From the analysis of this figure it can be said that, the lags between 1 and 8 of I_{fc} (short lags) are of great importance for the models, specially the 6^{th} lag as linear input, and the 7^{th} lag as a nonlinear input. In the case of I_{h1}, the important information is related with the lags between 6 and 15, that is the medium lags. Lag 15 appears in 19 of the 20 preferable individuals as nonlinear input, indicating that the information of this variable, 150 seconds in the past, is important for the models, and it is nonlinearly related with $T(k)$. In the same way, the 6^{th} lag of I_{h2} ($I_{h2}(k-6)$)appears also in 19 of the 20 preferable individuals as linear input. This lag is also important as a nonlinear input, given its presence in 15 preferable individuals. The lags 1 and 18 are also relevant as linear and nonlinear inputs, as well as lag 8 as linear input. The past memory of the system (lags of T), as expected, is of great importance as linear inputs, specially lags 1, 12, 14, and 17. The presence of 20 preferable individuals with lag 1 as input proves the physical validity of the system. The other lags show that the temperature 120, 140, and 170 seconds in the past is also important for the estimation of $T(k)$, again reflecting the thermal capacitance of the glycerin tank.

The presence of high absolute frequencies in the preferable set of some inputs, for example $T(k-1)$, $T(k-14)$, $I_{fc}(k-6)$, $I_{h1}(k-15)$, and $I_{h2}(k-6)$, and the presence of 8 NNs with 3 neurons, and 6 NNs with 5 neurons in the preferable set, indicates that MOGA converges to a group of individuals.

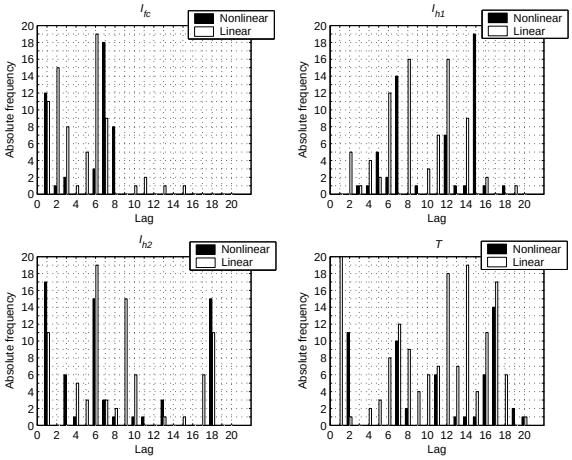

Fig. 4. Absolute frequency of the RBFLIC inputs (preferable set).

4.3 RBF and RBFLIC

Comparing both approaches hereby presented we may conclude that the best RBFLIC presents an increase in performance of approximately 22%, in agreement to the RMSEVs attained. The mean squared error is reduced from 0.0049 $(^oC)^2$ in the RBF case to 0.0032 $(^oC)^2$ in the RBFLIC case. The average error is also better in the RBFLIC case, a reduction in approximately 74% is obtained. However, the maximum absolute error is better in the RBF case, in approximately 0.1^oC. This contradiction is probably related with the presence of outliers. In terms of MCP, the best model in RBFLIC presents 69 parameters, against 61 in RBF run. This implies that the best RBF is less complex than the best RBFLIC in 8 parameters. This increase in RBFLIC complexity is related to the great number of linear inputs, given the reduced number of neurons in this model.

In general, the MOGA parametrisation presented in sub-section 3.3, applied to RBFLIC reached better results. In fact the RMSEV in the RBFLIC preferable set presents a medium value of 0.0018 with variance 1.6×10^{-7}, against 0.0025 with variance 2.37×10^{-7} in the RBF preferable set. This implies that the results achieved with the hybrid approach are in general 28% better. The success of the hybrid approach can be explained by the great linear component of the data. In this case a RBF NN with additional linear inputs performs better than a pure nonlinear RBF.
Comparing the results obtained in this work with the ones presented in (Simon *et al.*, 1998), it can be said that better results were achieved. The maximum absolute error was reduced from 0.44 $^oC$to 0.09^oC, the average error was reduced from -0.02$^oC$to -0.004^oC, and the mean squared error was reduced from 0.03$(^oC)^2$ to 0.0032$(^oC)^2$.

5. CONCLUSIONS & FUTURE WORK

The work hereby presented follows the work on punctual temperature modelling, published in (Teixeira *et al.*, 2004). The results reveals that a better performance is obtained for the MOGA parametrisation applied using a hybrid approach (RBFLIC), instead of using the normal approach (RBF). The increase in performance is approximately 28%. In addition, the best models obtained perform better than the best model in (Teixeira *et al.*, 2004). Although this work deals with punctual and invasive temperature estimation, the results point that better results should be obtained, in the same conditions of (Simon *et al.*, 1998), using this kind of methods. The temperature values used in this work (Table 1) are higher, representing the normal human temperature. At higher temperature values the transmission between mediums is higher, and more nonlinear properties arises. This imply that temperature modelling at low temperatures is more simple, and probably better performed by the RBF(LIC).
For future work it is suggested the use of B-Splines NN to approach this problem. This NN use different basis functions through the input space, locally adjusting itself to the problem.
It is also suggested for future work, to attempt modelling of temperature in time and space. This is a fundamental step in order to obtain feedback information for therapeutic ultrasound instrumentation control.

ACKNOWLEDGEMENTS

The authors gratefully acknowledge the financial support of: Fundação para a Ciência e a Tecnologia (scholarship SFRH/BD/1461/2003), and Conselho Nacional de Desenvolvimento Científico e Tecnológico (CNPq/CYTED 490.013/03-1), Brazil. The authors also acknowledge Eng. Pedro Frazão for the code used, and for some interesting discussions about the results obtained. Finally, acknowledgements to Hector Gomez, Guillermo Cortela and Carlos Negreira (Laboratorio de Acústica Ultrasonora, Universidade de la República, Uruguay), for the help in real data collection.

REFERENCES

Billings, S. and Q. Zhu (1993). Nonlinear model validation using correlation tests. Research report nº 463. Department of Automatic Control and Systems Engineering, University of Sheffield. Sheffield S14DU, UK.

Billings, S. and W. Voon (1986). Correlation based model validity tests for non-linear models. *International Journal of Control* **44**(1), 235–244.

Chinrungrueng, Chedsada and Carlo H. Séquin (1995). Optimal adaptive k-means algorithm with dynamic adjustment of learning rate. *IEEE Transactions on Neural Networks* **6**(1), 157–169.

Ferreira, P. M., A. E. Ruano and C. M. Fonseca (2003). Genetic assisted selection of rbf model structures for greenhouse inside air temperature prediction. In: *Proc. IEEE Conference on Control Applications*. Vol. 1 and 2. Istambul, Turkey. pp. 576–581.

Ferreira, P.M., E.A. Faria and A.E. Ruano (2002). Neural network models in greenhouse air temperature prediction. *Neurocomputing* **43**(1-4), 51–75.

Fonseca, C. M. and P. J. Fleming (1993). Genetic algorithms for multi-objective optimization: Formulation, discution and generalization. In: *Proc. 5th Int. Conf. Genetic Algorithms* (S. Forrest, Ed.). pp. 416–423.

Seip, Ralf, Philip VanBaren, Charles A. Cain and Emad S. Ebbini (1996). Noninvasive real-time multipoint temperature control for ultrasound phased array treatments. *IEEE Transactions on Ultrasonics, Ferroelectrics, and Frequency Control* **43**(6), 1063–1073.

Simon, C., P. VanBaren and E. S. Ebbini (1998). Two-dimensional temperature estimation using diagnostic ultrasound. *IEEE Transactions on Ultrasonics, Ferroelectrics, and Frequency Control* **45**(4), 1088–1099.

Teixeira, C. A., G. Cortela, H. Gomez, M. G. Ruano, A. E. Ruano, C. Negreira and W. C. A. Pereira (2004). Modelos de temperatura de um meio homogéneo sob ultrassom de terapia. Acepted to be published in the III CLAEB proceedings, 22-25 Sept. João Pessoa-PB, Brasil.